Mapping of mobile charges on insulator surfaces with the electrostatic force microscope

K. Domanský,[a] Y. Leng, and C. C. Williams
Department of Physics, University of Utah, Salt Lake City, Utah 84112

J. Janata
Molecular Science Research Center, Pacific Northwest Laboratory, Richland, Washington 99352

D. Petelenz
Hedco Microfabrication Facility, University of Utah, Salt Lake City, Utah 84112

(Received 8 April 1993; accepted for publication 28 June 1993)

Migration of surface ions in lateral fields on insulator surfaces may modify the electrical characteristics of underlying semiconductor structures causing device instabilities. A high sensitivity electrostatic force microscope is used to image the movement and spatial distribution of surface ions on Si_3N_4. Mobile surface ions are distributed by the fringing fields of a *p-n* junction and an open-gate field-effect transistor. The surface charge distribution and topography are imaged simultaneously on a micrometer scale.

When there is a lateral field present on an external insulator surface containing mobile ions, the ions migrate. The lateral field can be created by the fringing field of a *p-n* junction, an open-gate field-effect transistor (FET), a voltage biased metal line on the insulator surface, a biased scanning probe tip positioned close above the insulator, or even by charged species placed on the insulating surface.

Previously, force microscopy was used to image localized charge that was deposited on insulator surfaces by contact electrification or corona discharge.[1–4] In this letter, we demonstrate the capability of the electrostatic force microscope (EFM) to image the migrating surface ions on Si_3N_4 in fringing lateral fields.

The presence of mobile ions on the surfaces of semiconductors was postulated in the early 1950's.[5] It was observed that the mobility of surface ions was sensitive to ambient conditions, especially the presence of water vapor. Atalla *et al.*[6] presented a model in which the fringing field of a *p-n* junction under reverse bias separates positive and negative ions on the oxidized surface. The accumulated ions may modify the surface potential of the underlying silicon and change the device characteristics. Atalla's surface charge model was supported by Shockley *et al.* Using a Kelvin probe (KP) they measured effective contact potential differences along oxide-covered specimens with a *p-n* junction and an exposed electrode.[7,8] A smaller KP was employed in later studies[9] of ion accumulation and decay over a *p-n* junction as a function of surface chemical treatment. Schlegel[10] demonstrated surface-ion effects produced by a biased electrode buried between insulator layers in a region remote from the exposed electrode. This experiment showed that the buildup of surface ions does not require charge flow from the electrode. Studies[11–13] describe the effects of the surface ion migration on the characteristics of MIS capacitors.

In the past, the migration of surface ions was the cause of significant instabilities of discrete semiconductor devices and ICs. These problems were minimized by proper device design, using diffused channel stoppers and effective passivation and encapsulation.[14] However, these approaches cannot always be employed. Some FET based chemical sensors such as the surface accessible FET,[15] the perforated gate FET,[16] or the suspended gate FET[17] suffer from a strong drift due to ion migration. These devices cannot be sealed in hermetic packages because the chemical species must be allowed to penetrate into the gate area in order to produce a measurable response. From the viewpoint of these applications, mapping of surface-ion distributions with the EFM can provide useful information for the device designer, especially when there are doubts about the origin of the macroscopically observed drift. Moreover, the probe tips of nanometer scale radius in the EFM give much better resolution than the above KP with tip diameters of tens of micrometers.

Surface-ion accumulation can also cause problems while studying in air the charge distribution on insulator surfaces with scanning probes that utilize dc biased tips or when measuring local capacitance.[18] It should be pointed out that once a sample such as an oxidized silicon wafer is exposed to water vapor or other polar molecules, the screening effect of the surface ions may remain even if the sample is transferred into high vacuum.

A block diagram of the EFM is shown in Fig. 1. The instrument is a modified noncontact mode atomic force microscope (AFM).[2,3,19] A reflective glass cantilever with an electrochemically etched tungsten tip is mounted on a piezoelectric bimorph and vibrated at its resonant frequency ω_0. When the tip approaches the sample, the force gradient of the tip-sample interaction modifies the effective spring constant of the cantilever, resulting in both a resonant frequency shift, and a vibration amplitude reduction at the drive frequency. The motion of the tip is monitored by a differential interferometric detection system, with a sensitivity of about 10^{-4} Å/$\sqrt{\text{Hz}}$. A feedback loop adjusts the height of the tip to keep the vibration amplitude constant during a scan. The movement of the piezotube in the *z* direction represents the corresponding topography of the sample surface. At the same time, a sinusoidal voltage is

[a]Present address: Hedco Microfabrication Facility, University of Utah, Salt Lake City, UT 84112. Author to whom correspondence should be addressed.

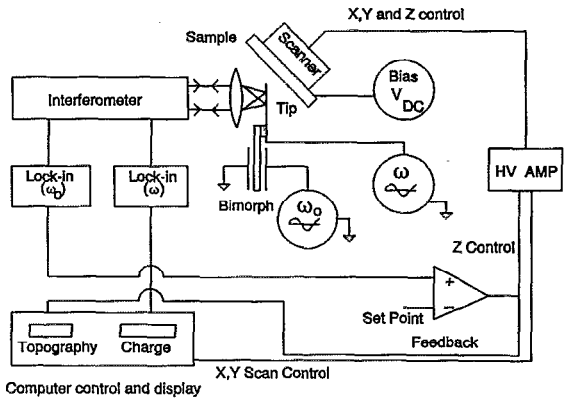

FIG. 1. Block diagram of the electrostatic force microscope.

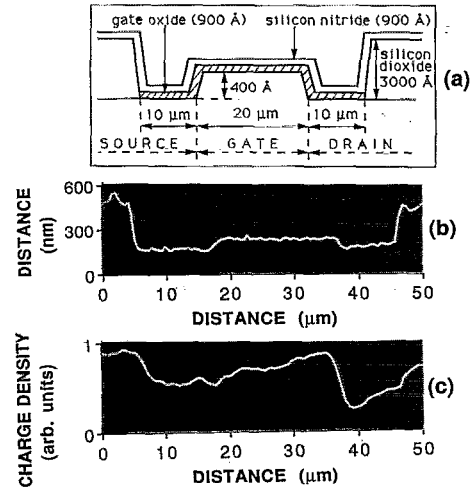

FIG. 2. An open-gate FET. (a) A cross section with the geometrical dimensions determined by the profilometer. The drawing is not to scale. (b) An individual topographic line scan from the image in Fig. 3. (c) An individual surface charge density line scan from the image in Fig. 3(b).

supplied to the tip at radian frequency ω. The applied voltage creates an electrostatic force between the tip and the sample, which is detected at frequency ω by a lock-in amplifier. This force has two components, one component depends on the local dielectric constant, the other component is proportional to the local surface charge variation. In this work, the dielectric constant variations are assumed to be small. Therefore, we attribute the measured EFM signals to the near-surface charge density. In these experiments, the frequency of the ac voltage applied to the tip is 5.50 kHz and the amplitude is 10 V. The cantilever has a resonant frequency of 5.17 kHz and an estimated spring constant of 100 N/m. The tungsten tip radius was estimated to be 50 nm and the tip-sample distance approximately 5 nm.

The specimens used in this study have structures similar to a MOSFET without the metal gate. The substrate used is p type, with 15 Ω cm resistivity. Sheet resistance of the phosphorus-doped source-drain regions is 25 Ω/□. The gate oxide was thermally grown. The top Si_3N_4 was produced by atmospheric pressure chemical vapor deposition from ammonia and silane at 870 °C. A cross section of the open-gate FET is shown in Fig. 2(a). The channel length defined by the diffusion mask is 20 μm.

EFM images of the open gate FET and the p-n junction are illustrated in Figs. 3 and 4. The charge image in Fig. 3(a) was taken after the chip was exposed at 25% relative humidity for 2 days with the source, drain, and substrate grounded. The sample was dried in N_2 prior to imaging. The charge image therefore represents the initial equilibrium condition when the surface ions redistribute themselves and cancel the fringing built-in fields of the p-n junctions. Next, a bias of +10 V was applied to the drain. Then, water vapor was introduced to increase the surface ion mobility. While the bias was still applied, the bubbler was bypassed and the chip was exposed to dry N_2 for 1 h. Subsequently, the bias was removed and the redistributed surface ions were imaged with all leads grounded as before [see Fig. 3(b)]. Individual topographic and charge line scans from this image are shown in Figs. 2(b) and 2(c). From these electrostatic force measurements, we estimate the surface charge density variation across the channel to be on the order of 10^{-9} C/cm^2.

A similar experiment was performed on the same chip with a p-n junction. Under wet N_2, a bias of +20 V was applied to the drain while the substrate was grounded and the source was left floating. After drying, the bias was removed, all leads were grounded, and the image shown in Fig. 4 was taken. Individual topographic and charge line scans of the p-n junction are illustrated in Figs. 5(a) and 5(b). After these measurements, wet N_2 was applied again with all leads grounded, and the charge signal was restored to its initial condition in less than 1 h (uniform signal over the entire region).

For an applied drain-to source voltage of 10 V, the open-gate depletion n-channel FET operates above the pinch-off point. This mode of operation is characterized by a surface depletion region formed at the drain end of the channel as illustrated in Fig. 6. Consequently, the lateral field on the insulator surface above the channel is produced by the voltage impressed across the surface depletion re-

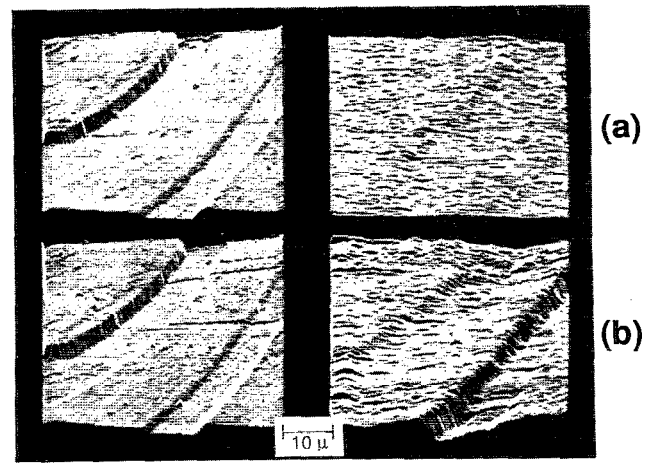

FIG. 3. 50 μm×50 μm EFM images of the open-gate FET. The images on the left-hand side represent topography, the images on the right-hand side represent surface charge density. All leads were grounded while imaging. (a) The initial equilibrium condition, (b) after 1 h of bias and wet conditions.

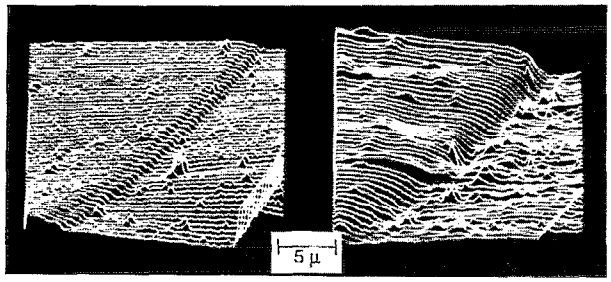

FIG. 4. 20 μm$\times$20 μm EFM images of a *p-n* junction, taken after 1 h of wet conditions and a bias of 20 V. The image on the left-hand side is topographic, the image on the right-hand side represents surface charge density. All leads were grounded during imaging.

gion. The lateral field is also created by the nonuniform free-carrier concentration in the channel. The strong lateral field of the depletion region sweeps the positive ions above the channel where they drift toward the source. This excess positive charge over the channel sets up an electric field across the gate insulator. As a result, conduction band electrons are attracted to the silicon surface. The decreased resistance of the channel will result in the increase of the saturation current which in turn produces a higher voltage drop across the surface depletion region. Consequently, the fringing field of the depletion region will increase and the process of the charge separation on the insulator surface will accelerate. While the positive ions are drifting towards the source, the negative ions migrate in the opposite direction. Since in the drain region, no significant lateral field exists, the tail of the negative ion pileup is steeper and shorter than that over the channel [see Fig. 2(c)].

During these experiments, the average movement of surface ions was observed independently by monitoring the change in the saturation drain current in the device under bias. From the monitored change of the saturation drain current (by 100 μA) from the original value of 600 μA, it is possible to estimate the change of the average net charge density over the channel. Taking into account the fixed charge density in the oxide and the dielectric constants of oxide and nitride layers, one arrives at an estimate of the displaced charge density of 5×10^{-9} C/cm^2.

The mechanism of charge separation over a *p-n* junction has been already described.[6,20] The charge distribution

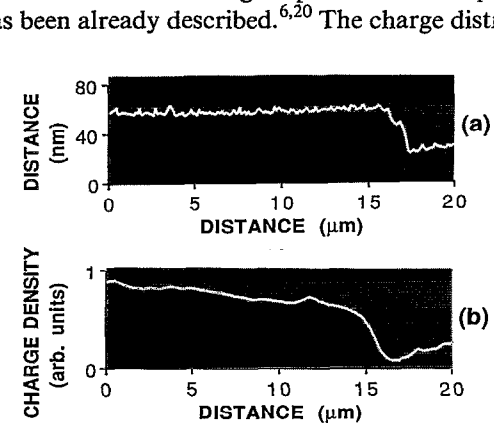

FIG. 5. Individual topographic (a) and surface charge density (b) line scans from the image in Fig. 4.

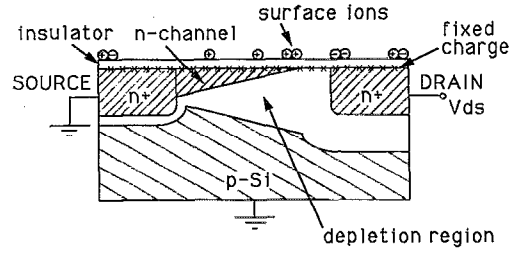

FIG. 6. Simplified schematic diagram of an *n*-channel open-gate FET operated above the pinch-off point.

over the *p-n* junction in Fig. 5(b) resembles the distribution obtained previously with a KP,[7] but on a much smaller scale (micrometers instead of millimeters). The differences may be attributed to the dissimilarities in the experimental and sample conditions (humidity, insulator thicknesses, ion mobilities on silicon nitride, and silicon dioxide surfaces and substrate doping levels).

In conclusion, we have imaged by EFM surface ions which migrate on an external insulator surface under the influence of lateral electric fields. The EFM has been shown to be a useful tool for studying the role that surface ions play in operational open gate FET structures.

We thank L. E. Thomas and R. J. Huber for useful comments. The work was supported by the subcontract to Hedco from the Pacific Northwest Laboratory and Center for Biopolymers at Interfaces at the University of Utah.

[1] J. E. Stern, B. D. Terris, H. J. Mamin, and D. Rugar, Appl. Phys. Lett. **53**, 2717 (1988).
[2] B. D. Terris, J. E. Stern, D. Rugar, and H. J. Mamin, Phys. Rev. Lett. **63**, 2669 (1989).
[3] C. Schönenberger and S. F. Alvarado, Phys. Rev. Lett. **65**, 3162 (1990).
[4] C. Schönenberger, Phys. Rev. B **45**, 3861 (1992).
[5] W. L. Brown, Phys. Rev. **91**, 518 (1953).
[6] M. M. Atalla, A. R. Bray, and R. Linden, Suppl. Proc. Inst. Electron. Eng. (London) Pt. B **106**, 1130 (1958).
[7] W. Shockley, H. J. Queisser, and W. W. Hooper, Phys. Rev. Lett. **11**, 489 (1963).
[8] W. Shockley, W. W. Hooper, H. J. Queisser, and W. Schroen, Surf. Sci. **2**, 277 (1964).
[9] W. Schroen, RADC Ser. Reliability, Phys. Failure Electron. **4**, 291 (1966).
[10] E. S. Schlegel, R. S. Keen, and G. L. Schnable, in *Proceedings of the 8th International Reliability Physics Symposium* (IEEE, New York, 1970), p. 9.
[11] P. O. Ho, K. Lehovec, and L. Fedotowsky, Surf. Sci. **6**, 440 (1967).
[12] R. F. Pierret and D. W. Small, IEEE Trans. Electron Devices **ED-20**, 457 (1973).
[13] B. Joseph, Phys. Status Solidi A **45**, K25 (1978).
[14] N. E. Lycoudes and C. C. Childers, IEEE Trans. Reliability **R-29**, 237 (1980).
[15] M. Sternberg and B. I. Dahlenback, Sensors and Actuators **4**, 273 (1983).
[16] I. Ludström and D. Söderberg, Sensors and Actuators **2**, 105 (1981).
[17] M. Josowicz and J. Janata, *Suspended Gate Field Effect Transistor in Chemical Sensor Technology*, edited by T. Seiyama (Kodansha, Tokyo, 1988), Vol. I, p. 153.
[18] Y. Huang and C. C. Williams, in *Proceedings of the Second International Workshop on the Measurement and Characterization of the Ultrashallow Dopant Profiles in Semiconductors*, edited by R. Subrahmanyan, C. Osborn, and P. Rai-Choudhury (MCNC, Research Triangle Park, NC, 1993), Vol. 2, p. 286.
[19] Y. Leng and C. C. Williams, SPIE Proc. 1855, 35 (1993).
[20] E. D. Metz, RADC Ser. Reliability, Phys. Failure Electron. **2**, 163 (1964).